Géographie physique et Quaternaire

Energy Exchange During River Icing Formation in a Subarctic Environment, Yukon Territory
Les échanges d'énergie pendant la formation de nappes de glace dans les cours d'eau subarctiques, Territoire du Yukon
Energie-Austausch während der Bildung von Flusseis in subarktischem Milieu, Yukon Territorium

Xiaogang Hu, Wayne H. Pollard and John E. Lewis

Explore this journal

Cite this article

Article abstract

Icings are common hydrologic phenomena in cold subarctic environments. They are formed by the accumulation of repeated overflow layers during winter. The size and thickness of the icing layers, however, are determined by the interaction of surface water hydrologic and microclimatologic systems. This paper examines the energy exchanges associated with icing layers with different thicknesses. In the case of thick layers of overflow, ice layers require a longer time to freeze completely due to greater latent heat stored in larger water volumes. Milder air temperatures will slow growth even further. Under such conditions, flowing water between the top ice cover and the underlying ice body provides significant amounts of energy. As much as 60-87 % of the energy may be supplied by running water. Under progressively colder temperature conditions, faster growth rates reduce the time of water flow and, therefore, reducing the relative amount of energy supplied by flowing water. In this case energy is provided mainly by the latent heat released by the freezing of water contained in the overflow layer. Under certain conditions, the absorption of solar radiation also generates a considerable amount of energy input to the regime. This energy is released mostly through sensible and radiative heat losses. During icing layer formation, latent heat is the least important, accounting for only 6-17 % of the total heat loss.

ENERGY EXCHANGE DURING RIVER ICING FORMATION IN A SUBARCTIC ENVIRONMENT, YUKON TERRITORY

Xiaogang HU*, Wayne H. POLLARD and John E. LEWIS, Department of Geography and Centre for Climate and Global Change Research, McGill University, 805 Sherbrooke Street West, Montréal, Québec H3A 2K6.

ABSTRACT Icings are common hydrologic phenomena in cold subarctic environments. They are formed by the accumulation of repeated overflow layers during winter. The size and thickness of the icing layers, however, are determined by the interaction of surface water hydrologic and microclimatologic systems. This paper examines the energy exchanges associated with icing layers with different thicknesses. In the case of thick layers of overflow, ice layers require a longer time to freeze completely due to greater latent heat stored in larger water volumes. Milder air temperatures will slow growth even further. Under such conditions, flowing water between the top ice cover and the underlying ice body provides significant amounts of energy. As much as 60 - 87 % of the energy may be supplied by running water. Under progressively colder temperature conditions, faster growth rates reduce the time of water flow and, therefore, reducing the relative amount of energy supplied by flowing water. In this case energy is provided mainly by the latent heat released by the freezing of water contained in the overflow layer. Under certain conditions, the absorption of solar radiation also generates a considerable amount of energy input to the regime. This energy is released mostly through sensible and radiative heat losses. During icing layer formation, latent heat is the least important, accounting for only 6 - 17 % of the total heat loss.

RÉSUMÉ *Les échanges d'énergie pendant la formation de nappes de glace dans les cours d'eau subarctiques, Territoire du Yukon.* La formation de nappes de glace stratifiée est un phénomène hydrologique courant en milieu subarctique. Il résulte de l'accumulation d'écoulements successifs pendant l'hiver. La taille et l'épaisseur des couches de glace sont déterminées par l'interaction entre les systèmes microclimatologique et hydrologique de l'eau de surface. On étudie ici les échanges d'énergie suivant différentes épaisseurs de nappes de glace. Dans le cas d'épaisses nappes d'écoulement, les couches de glace prennent plus de temps à geler entièrement en raison de la plus grande quantité de chaleur latente emmagasinée dans les volumes d'eau. Des températures de l'air plus douces vont davantage ralentir le processus. Dans de telles conditions, l'eau circulant entre le couvert de glace supérieur et la glace sous-jacente procure des quantités d'énergie appréciables. De 60 à 87 % de l'énergie est fournie par l'eau libre. Avec des températures progressivement plus froides, l'englaciation accélérée réduit le temps d'écoulement de l'eau, diminuant ainsi la quantité relative d'énergie fournie par l'eau. Dans ce cas, l'énergie est livrée par la chaleur latente libérée par le gel de l'eau contenue dans la couche de débordement. Dans certaines conditions, l'absorption du rayonnement solaire produit aussi une quantité considérable d'entrée d'énergie dans le régime thermique. Cette énergie est libérée par l'entremise de pertes appréciables de chaleur irradiante. Pendant la formation d'une nappe de glace, la chaleur latente est la moins importante, ne comptant que pour 6 à 17 % de la perte totale de chaleur.

ZUSAMMENFASSUNG *Energie-Austausch während der Bildung von Flusseis in subarktischem Milieu, Yukon Territorium.* Die Bildung von Eisschichten ist ein verbreitetes hydrologisches Phänomen in kaltem subarktischem Milieu. Sie entstehen durch Akkumulation sukzessiver Überlaufschichten während des Winters. Die Größe und Dicke der Eisschichten wird durch die Interaktion der hydrologischen und mikroklimatologischen Systeme des Oberflächenwassers bestimmt. In diesem Beitrag wird der Energieaustausch in Verbindung mit Eisschichten unterschiedlicher Dicke untersucht. Im Falle dicker Überlaufschichten brauchen die Eisschichten mehr Zeit, um komplett zuzufrieren, wegen der größeren latenten Wärme, die in größeren Waservolumen gespeichert ist. Mildere Lufttemperaturen verlangsamen den Prozess sogar noch mehr. Unter solchen Bedingungen liefert das zwischen der Oberflächeneisschicht und dem darunter liegenden Eiskörper fließende Wasser beträchtliche Mengen an Energie. 60 bis 87 % der Energie kann durch fließendes Wasser geliefert werden. Unter progressiv kälteren Bedingungen wird die Geschwindigkeit des Wasserflusses durch die beschleunigte Vereisung reduziert, und infolgedessen auch die durch das fließende Wasser gelieferte relative Energiemenge. In diesem Fall wird die Energie hauptsächlich durch die latente Wärme geliefert, die durch das Einfrieren des in der Überlaufschicht enthaltenen Wassers freigesetzt wird. Unter gewissen Umständen produziert auch die Absorption von Sonnenstrahlen eine beträchtliche Menge von Energie-Eingabe in das System. Diese Energie wird vor allem durch beträchtliche ausstrahlende Wärmeverluste befreit. Während der Bildung der Eisschicht ist die latente Wärme am wenigsten wichtig und betrifft nur 6 - 17 % des totalen Wärmeverlusts.

LIST OF SYMBOLS

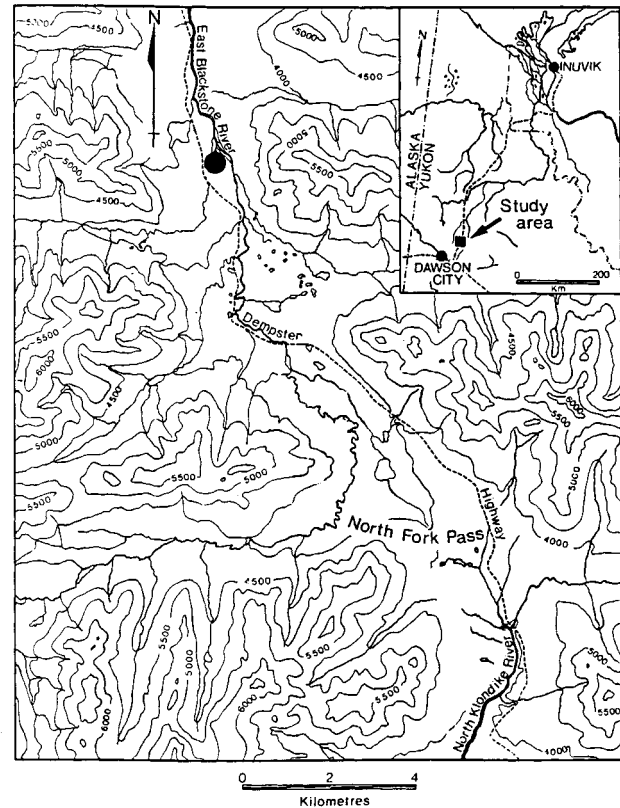|	
c_i	specific heat of ice
C_p	specific heat of air at constant pressure
e_s	saturation vapour pressure over water
e_i	saturation vapour pressure over ice
g	acceleration due to gravity
h_i	thickness of icing layer
h_w	thickness of water layer
H	depth of underlying ice
H_c	total amount of conductive heat
k	von Karmen's constant; lag in spatial or temporal series
K_{ice}	thermal conductivity of ice
K_b, K_s, K_w	bulk heat exchange coefficients
L	latent heat of fusion (open water period) or sublimation (ice covered period)
q_a	specific humidity of the air
q_s	specific humidity above ice surface
Q_e	latent heat flux
Q_h	sensible heat flux
Q_{il}	heat flux conducted from underlying ice
Q_{iu}	heat flux conducted through top layer of ice
Q_s	incoming short wave radiation at the surface of ice or snow
Q_{sa}	solar radiation absorbed by icing layer
Q_{si}	solar radiation reaches the snow-ice interface
Q_{sp}	solar radiation penetration at depth h_i+h_w
Q_{spl}	internal heating at the lower ice-water interface
Q_{spu}	internal heating at the upper ice-water interface
$Q_{sp(w+i)}$	internal heating caused by absorption of solar radiation of both water and ice layers
Q_w	total heat from water
Q_{wf}	heat released by freezing of still water
Q_{wr}	heat recharged by flowing water
Q^*	net radiation
ΔQ	heat storage
R_b	bulk Richardson number
t	time
T_a	air temperature
T_f	mean temperature of icing layer at the end of a cycle
T_i	mean temperature of icing layer at beginning of a cycle
T_{ice}	mean temperature of icing layer
T_s	surface temperature
U_a	wind speed at the height of Z
U_a	wind speed at the surface of icing
Z	height of the measurement
z_0	roughness length of the icing surface
α	albedo
β_i, β_s and β_w	bulk extinction coefficients of ice, snow and water
ρ_a	density of air
ρ_i	density of ice
ρ_w	density of water

FIGURE 1. The location of the study area. Balck dot indicates the icing site.

Localisation de la région à l'étude. Le point noir donne l'emplacement de la formation de nappes de glace

INTRODUCTION

This paper focuses on the analysis of the energy balance associated with the formation of icing layers of different thicknesses under a range of climatic conditions. The energy exchanges during icing layer formation, the components of the energy balance for icing cycles, and the temporal variations of energy fluxes during formation of single or doubled icing layers, are discussed. Field work was conducted in the North Fork Pass area of Yukon Territory in Canada (Fig. 1).

Icings are sheet-like masses of layered ice, formed on either the ground or river ice surfaces, by the repeated overflow of ground or surface water. Depending on the water source, three types of icings are generally recognized: river icings, ground icings and spring icings (Akerman, 1980; Carey, 1973; Pollard and van Everdingen, 1992; Sokolov *et al.*, 1989). Large icings are found in many small streams and shallow rivers in subarctic environments where discharge persists throughout the winter.

The importance of icings to water resources research and their impact on northern engineering structures have been the focus of many studies (Carey, 1973; van Everdingen, 1982; Kane, 1981; Slaughter, 1990; Sokolov, 1978). River icings may modify the hydraulic geometry of river channels, creating significant changes in fluvial geomorphology (Froehlich and Slupik, 1982). Of particular hydrologic importance

is the fact that river icings temporarily store winter discharge, redistributing it during spring and summer. It is impossible to accurately estimate northern water resources in terms of both spatial and temporal distribution without considering the contribution from various icing sources (van Everdingen, 1990). Icings also present a series of unique problems for highways, railways, pipelines and airstrips. The prevention of icings and the maintenance of structures affected by icings are costly in areas with cold climates.

Despite extensive literature on icings, the nature of the energy exchange during icing formation and the feedback mechanism of the surface energy balance that influences the release of water prior to the development of a new layer of ice remains unclear. In particular, there is little information concerning the energy balance during icing layer formation for different climatic conditions. For example, Gavrilova (1972) undertook an analysis of the seasonal energy balance of icing bodies, however, he did not address the energy exchange during individual overflow events or icing layers formation. The study that is closest to our investigation is the analysis of heat exchanges of ice layers during ice platform construction in the High Arctic by Nakawa (1980). Nakawa addressed a problem similar to that of icing formation, except that water layers are treated as static and the ice layers in his study were very thin (<1.6 cm). Since the ice layers studied by him involve saline (sea) water sprayed on the platform surface, there remains a significant departure from natural icing systems, physically and hydrologically. Furthermore, the air temperatures were very cold (T_{mean}< -28 °C) and, because of the high latitude and time of the year, there was no short wave radiation involved in his study. By comparison, river icing formation involves larger and more continuous discharge, and icing layers are usually much thicker than the ice layers examined by Nakawa. The greater overflow depths produce thicker

icing layers which require longer time to freeze and, as a result, the energy contribution from flowing water cannot be ignored. This is especially the case when air temperatures are closer to freezing point. Depending upon latitude, solar radiation in subarctic areas generally takes on increasing importance from the middle of February onwards, when icings are still very active (Kane and Slaughter, 1972).

STUDY AREA AND DATA COLLECTION

STUDY AREA

This study is based on observations of a moderate-sized river icing in the North Fork Pass area of the Ogilvie Mountains, north-central Yukon Territory (Fig. 1). The climate of the area is dominated by long cold winters and relatively low precipitation. Summers are short, damp and cool. Dawson City airport (64° 04'N, 139° 50'W; 253 m asl), the nearest meteorological station, is located about 60 km to the southwest of the study site. The mean annual air temperature at Dawson is -4.9 °C, and the mean monthly temperature for January is as low as -28.7 °C. Because of the higher elevation, the temperature of the study area is colder than that of Dawson City, the annual mean temperature of -7.5 °C is estimated by Pollard (1983) for the North Fork Pass area. At Dawson City airport, the mean annual precipitation is only 326 mm with 41 % of the total falling during summer months (Environment Canada, 1950-1990). The mean daily air temperature in the study area is highly variable. Figure 2 shows that the air temperature can vary from above -10 °C to lower than -40 °C during icing growth. Permafrost is known to be discontinuous in the Dawson area, however the cooler conditions in North Fork Pass may produce locally continuous permafrost conditions, especially in the high mountain regions (Pollard 1983).

FIGURE 2. Winter mean daily air temperature in the East Blackstone River valley (1993-1994).

La température moyenne de l'air en hiver dans la vallée de l'East Blackstone (1993-1994).
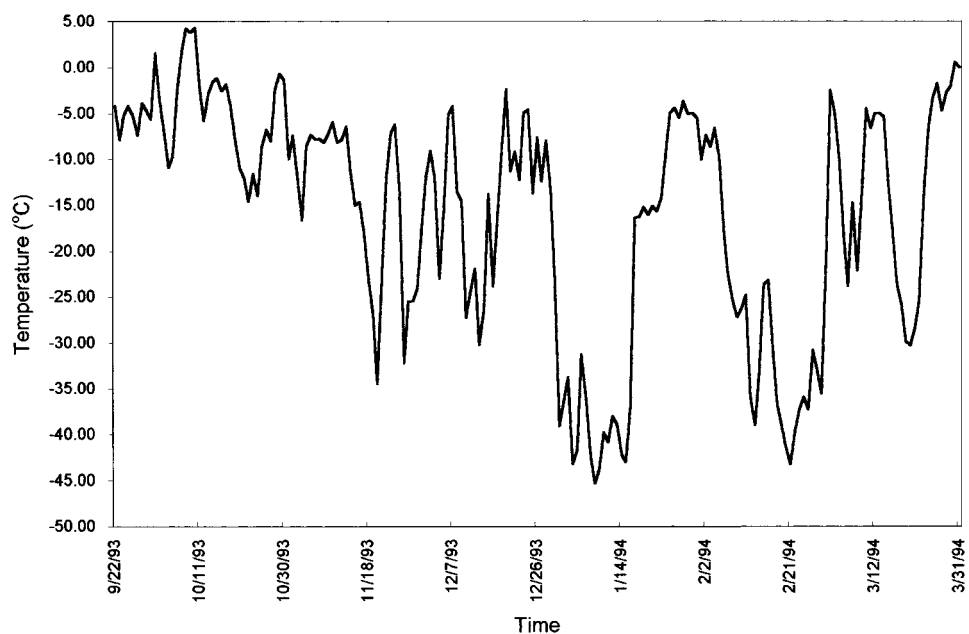
During the Pleistocene, this region experienced at least three advances of valley glaciers that eroded the main valley and deposited a series of moraines (Pollard, 1983). Hence, the valley floors of this region are covered by glacial till and glaciofluvial sediments. Ground water systems are well developed and provide streams with sufficient baseflow to sustain discharge throughout the year. Ground water recharge is believed to occur during the summer through the melting of snow, and through rainfall.

The East Blackstone River icing occurs annually in a wide braided section of the channel. The mean thickness, width and length of the icing in the winter of 1993-1994 were 1.6 m, 620 m and 640 m, respectively.

INSTRUMENTATION

An automatic meteorological station was set up in an area of frequent overflow. Wind speed, temperature and relative humidity were measured at 0.5 and 1.8 m above the ice surface using Campbell Met 1 wind speed sensors, 107 temperature and 207 RH sensors. The net radiation and incoming short-wave radiation were measured at a height of 1.0 m above the surface using a net radiometer and a pyranometer. Ice temperatures were measured at various depths within the ice using thermocouples (Type T). These thermocouples were placed 2 cm apart in the upper 10 cm of the ice, then 10 cm apart for next 20 cm and 20 cm apart to a depth of 50 cm prior to icing formation. The surface temperature of each icing layer was measured at 1 to 2 mm below the icing surface with thermocouples.

ICING PROCESSES

Icing growth involves the repeated overflow of water on the surface of an existing ice body. In general, overflow originates from three different sources: discharge through fractures in the ice body; discharge along stems of large plants protruding through the ice; and seepage from river banks. Of the three, the latter plays a very limited role, while the first two are of great importance. When water flows from a point source, a tension crack for instance, it occurs as a thin layer spreading in a down-slope direction. When the temperature of the water layer drops to the freezing point, a thin ice skin is formed. This ice skin thickens and eventually joins with the underlying ice. If water supply is continuous, it is observed that the hydraulic pressure will accumulate when the flow conduit is blocked by the growing ice cover. An icing blister may form around the point of discharge, and eventually rupture. Before the top layer is completely frozen, a second layer may form on top of it. A third layer, however, rarely forms during a single overflow event, since the water tends to flow into adjacent areas that lie at lower surface elevations. At a given point, therefore, icings are formed by the discontinuous accumulation of overflow layers. Figure 3 illustrates the sequence of processes during an icing layer formation.

The thickness of a single icing layer is influenced by the combination of weather, micro-topography, discharge, and water temperature. During the thickening process of the newly formed thin ice cover, continuous flow of water between the surface ice cover and underlying ice mass occurs. The ice skin is thus floating on a film of water and the thickness of the icing layer is increasing over time. It follows that severe cold temperatures accelerate the rate of ice growth, and result in a thinner layer; while thicker icing layers are produced under milder climatic conditions. The speed of water flow is controlled by a combination of factors, namely water temperature, surface energy flux processes, discharge of the water and the slope of the ice surface. This has been discussed in detail by Hu and Pollard (1998).

ENERGY EXCHANGES:
THEORETICAL CONSIDERATIONS

When an overflow event occurs, the temperature of the ice beneath the new icing layer is increased by the latent heat that is released during the freezing process. The energy is thus stored in the ice. When the icing layer is completely frozen, the energy storage of the ice underneath will gradually be released. In this paper, the cycle of an icing layer formation is defined by the energy storage in the ice underneath the icing layer. A cycle of icing layer formation begins when the water overflows on to the ice surface. The cycle is completed when the energy stored in the ice beneath the icing layer is completely dissipated, specifically when the vertical temperature profile in the underlying ice returns to the same distribution as prior to overflow. Three distinct time periods can be identified in the cycle: (a) the open water period; (b) the ice thickening period; and (c) the icing layer cooling period. The energy exchanges for each of the three periods are shown in Figure 4. It is clear that icing layer formation involves two ice-water interfaces: the upper interface propagates vertically downward, while the lower interface moves upward.

ICE GROWTH AT THE UPPER ICE-WATER INTERFACE

The growth of ice at the upper ice-water interface is defined by:

$$Q_{iu} - Q_w - Q_{spu} = \rho_i L\left(\frac{dh_i}{dt}\right) \tag{1}$$

where Q_{iu} is the energy flux through the top layer of ice (Wm^{-2}); Q_w is the energy flux from flowing water (Wm^{-2}); Q_{spu} is the internal heating at the upper ice-water interface caused by short wave radiation penetration (Wm^{-2}); D_i is the density of the ice (kg m^{-3}); L is the latent heat of fusion (J kg^{-1}); H represents the thickness of the ice growth (m) and t is the time (s).

ICE GROWTH AT THE LOWER ICE-WATER INTERFACE

The growth of ice at the lower ice-water interface can be written as:

$$Q_{il} - Q_w - Q_{spl} = \rho_i L\left(\frac{dh_i}{dt}\right) \tag{2}$$

where Q_{il} is the conductive heat flux from the underlying ice body; Q_w is the heat transfer from the water to the ice (Wm^{-2}); and Q_{spl} is the internal heating caused by the absorption of solar radiation at the lower ice-water interface.
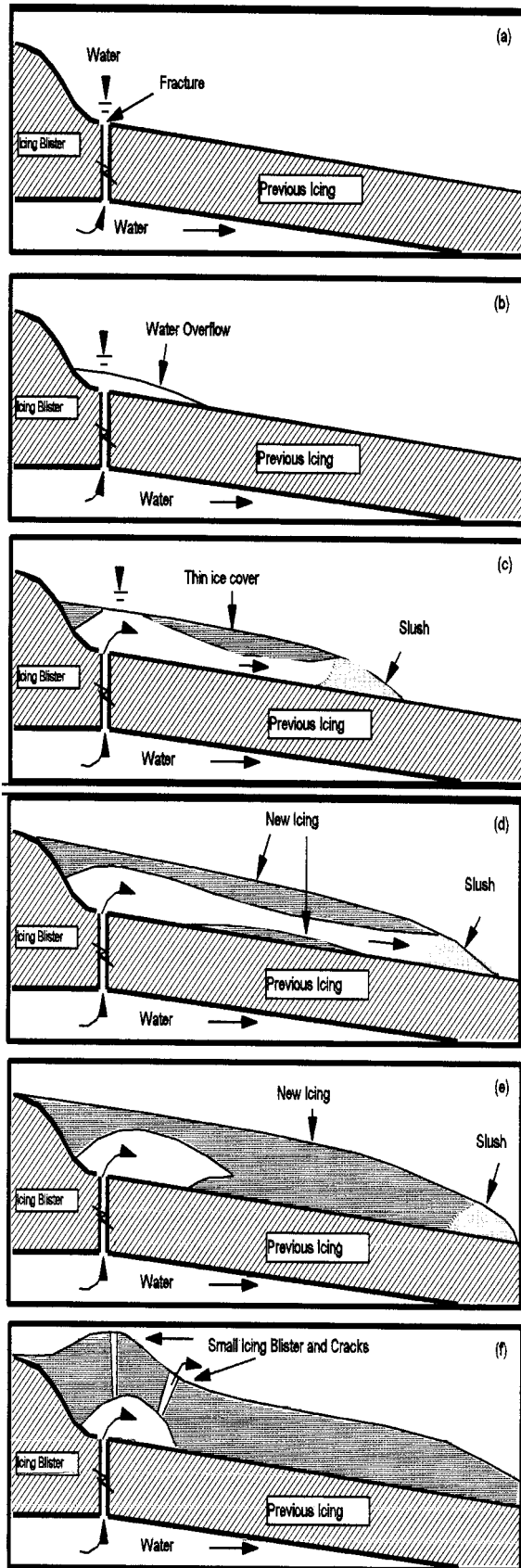
THE ENERGY BALANCE DURING ICING LAYER FORMATION

At any time during the icing formation, the energy balance of a new icing layer can be written as:

$$Q^* = Q_h + Q_e + Q_w + Q_{il} + Q_{sp(w+i)} + \Delta Q \tag{3}$$

where Q^* is the net radiation, which includes net shortwave radiation and net long wave radiation; Q_h is the sensible heat flux into the atmosphere from the surface of the ice/water; Q_e is the latent heat flux caused by evaporation (open water) or sublimation (ice); Q_w is the heat transferred by flowing water into the ice above and below it; $Q_{sp(w+i)}$ is the internal heating caused by the absorption of solar radiation by the ice and water layers; Q_{il} is the heat conduction from the underlying ice; and ΔQ is the change in energy storage within the layer as well as in the underlying ice during a time of Δt.

ENERGY EXCHANGE: THE DETERMINATION OF THE COMPONENTS

The sensible and latent heat fluxes, the heat conducted from the ice body, the energy transferred from solar radiation, the energy carried by flowing water, and the energy stored in the ice are estimated by the following methods.

SENSIBLE AND LATENT HEAT

The convective energy exchange between the atmosphere and ice is carried out through sensible and latent heat fluxes. These fluxes can be calculated by using an aerodynamic method, using measured profiles of wind speed, temperature and humidity close to the ice surface. Generally, Q_h and Q_e can be expressed in bulk form as follows:

$$Q_h = \rho_a C_p K_s (U_a - U_s)(T_a - T_s) \tag{4}$$

$$Q_e = \rho_a L K_w (U_a - U_s)(q_a - q_s) \tag{5}$$

where ρ_a is the density of the air; C_p is the specific heat under constant pressure; L is the latent heat of fusion (open water period) or sublimation (ice covered period); K_s and K_w are the bulk-exchange coefficients; U refers to wind speed; T is temperature; q refers to specific humidity above the ice surface; and the subscripts a and s designate measurements in the air and at the ice surface.

The exchange coefficients are calculated under the assumptions of a logarithmic wind profile, and the equality of the eddy coefficients (Kuhn, 1979; Munro and Davis, 1978),

FIGURE 3. The sequential development of an icing layer: (a) initial fracture of icing; (b) water emerges through the crack; (c) a thin ice skin starts to form; (d) ice cover is completed and is floating on a thin layer of flowing water; (e) the ice cover encounters the underlying ice; (f) the pressure accumulates forming a small icing blister, which then fractures to allow a new layer of icing to form.

La séquence de formation des nappes de glace : (a) fissure dans la nappe initiale de glace ; (b) écoulement d'eau par la fissure ; (c) début de formation d'une pellicule de glace ; (d) couvert de glace complété flottant sur une mince couche d'eau ; (e) contact entre le couvert de glace et la glace sous-jacente ; (f) accumulation de la pression jusqu'à formation d'un petit bombement, qui en vient à se fissurer, puis formation d'une nouvelle nappe de glace.
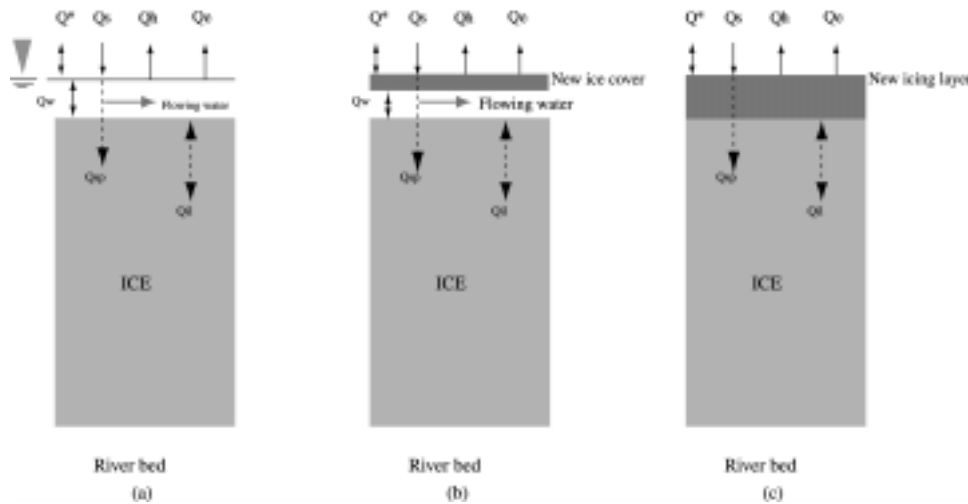
FIGURE 4. The energy exchange system during icing layer formation: (a) open water period; (b) ice cover thickening period; (c) new icing layer cooling period.

Le système d'échange d'énergie au cours du processus de formation d'une nappe de glace en trois périodes : (a) eaux libres ; (b) formation de la glace ; (c) refroidissement de la nappe de glace nouvellement formée.

adjusted by the bulk Richardson Number for stability. The bulk aerodynamic approach derives the bulk coefficient K_b as (Hay and Fitzharris, 1988):

$$K_b = K_s = K_w = \frac{k^2(1 - 5R_b)^2}{\left[\ln\left(\frac{Z}{z_0}\right)\right]^2} \tag{6}$$

for stable conditions and

$$K_b = K_s = K_w = \frac{k^2(1 - 16R_b)^{3/4}}{\left[\ln\left(\frac{Z}{z_0}\right)\right]^2} \tag{7}$$

for unstable conditions. Where k is von Karman's constant (0.40), Z is the measurement height, Z_0 is the roughness length and R_b is the bulk Richardson Number given by (Moore, 1983):

$$R_b = \frac{g(T_a - T_s)(Z - z_0)}{0,5(T_a + T_s)U_a^2} \tag{8}$$

where g is the acceleration due to gravity (m/s^2). The roughness length z_0 can be estimated using:

$$z_0 = e^{\left[\frac{U_2 \ln Z_1 - U_1 \ln Z_2}{U_1 - U_2}\right]} \tag{9}$$

where 1 and 2 denote two measurement heights. The roughness length is a highly variable parameter which is very sensitive to errors in wind speed measurement (Price and Dunne, 1976; Moore, 1983). Using two levels of wind speed measurement, and with three hundred and sixty wind speed profiles, we calculated a mean roughness length of $0.11*10^{-4}$ m for the icing surface. This length was used in the calculation of exchanges and compares favourably with that of Sutton (1953), who suggested a value of $z_0=0.1*10^{-4}$ m for a smooth ice surface. The parameters of air density (D_a), saturation vapour pressures over water (e_s) and ice (e_i), and the latent heat of sublimation (L_s), are all functions of temperature. The temperatures were divided into seven classes (0 to -5, -5 to -10, -10 to -15, -15 to -20, -20 to -25, -25 to -30 and < -30 °C) in their calculations and values of e_s, e_i and L_s

were taken from Rogers (1979). For the calculation of the latent heat flux, it was assumed that air was always saturated immediately above the ice surface. C_p is taken as 1010 J kg^{-1} K^{-1} (Oke, 1978). Given the short time period associated with icing layer formation, the atmospheric pressure was not measured at the site, but rather a measurement of daily atmospheric pressure from Dawson City was used, after adjusting for elevation.

ENERGY CONDUCTION

The temperature distribution in the underlying ice is not linear. Within a thin layer, however, the heat conduction can be linearly approximated and is controlled by the temperature gradient and the thermal conductivity of the ice:

$$Q_{il} = K_{ice} \frac{dT_{ice}}{dH} \tag{10}$$

where K_{ice} is the thermal conductivity of the ice; dT_{ice}/dH is the temperature gradient of the ice. K_{ice} is dependent mainly on temperature (and to a lesser extent on ice crystallographic orientation), and for practical purposes, the following equation, suggested by Yen (1981), is used to determine K_{ice}:

$$K_{ice} = 9,828 e^{-0,0057 T_{ice}} \tag{11}$$

where T_{ice} is in absolute temperature (°K).

ENERGY GENERATED BY SOLAR REDIATION

The penetration of short wave radiation is an important internal heating source during icing formation. In the field, however, it is difficult to directly measure the amount of energy penetrating the ice. Also, the penetration of solar radiation is strongly wave-length dependent, making it difficult, therefore, to accurately account for its input. Nevertheless, since the vertical distribution of solar heating in the ice is not the main topic of interest, we have estimated the transmission of solar radiation using Beer's law, an approach used by Maykut and Untersteiner (1971), and Shen and

Chiang (1984). The amount of shortwave radiation that penetrates the ice cover and the water layer to the lower boundary of an icing layer is defined by:

$$Q_{sp} = Q_s(1-\alpha)e^{-(\beta_i h_i + \beta_w h_w)} \tag{12}$$

where Q_{sp} is the intensity of the shortwave radiation at depth $h_i + h_w$; Q_s is the incoming shortwave radiation at the icing surface; is the albedo of the ice; β_i and β_w are the bulk extinction coefficients for ice and water respectively; and h_i and h_w are the thickness of the ice layer and water layer, respectively. Theoretically b_i and b_w are different. Since the total thickness of an icing layer is generally less than 10 cm, most of the time we are dealing with ice alone rather than water or both water and ice. Moreover, due to the small difference in the refractive indices of ice and water (Perovich and Grenfell, 1982), a bulk extinction coefficient of β_i=3.1 m^1 for solar radiation in bubbly ice (Hobbs, 1974) is used in this study. The heat flux received for the icing layer can thus be simplified as:

$$Q_{sa} = Q_s(1-\alpha)-Q_s e^{-\beta_i h_i} \tag{13}$$

where Q_{sa} is the heat flux absorbed by an icing layer and h_i is the thickness of the icing layer. For freezing ice, which is close to slush ice, a value of 0.41 is used for albedo (Bolsenga, 1969).

ENERGY FLUX FROM FLOWING WATER AND ENERGY STORAGE

During the formation of a river icing layer, a thin ice cover is floating on a film of running water, and the freezing process therefore proceeds much more slowly than in the case of still water. The running water supplies energy not only at the beginning of the icing layer formation, but also throughout its thickening period. The heat contribution from the running water is, therefore, very significant. It is, however, difficult to directly calculate the heat flux from the water to the ice cover during icing layer growth. Nevertheless, the combination of both Q_w and ^aQ can be calculated from the residuals of equations (3), (4) and (5) so that:

$$Q_w + \Delta Q = Q^* - (Q_h + Q_e + Q_{sa} + Q_{il}) \tag{14}$$

For a full icing cycle, we can derive:

$$\int(Q_w + \Delta Q)dt = \int[Q^* - (Q_h + Q_e + Q_{sa} + Q_{il})]dt \tag{15}$$

The positive amount of heat stored during the first and second periods will be released during the third period. At the end of an icing cycle, according to the definition given previously, $\int\Delta Q dt \Rightarrow 0$. The heat input from water (Q_w) consists of two parts, one part being the heat released by the freezing of still water (Q_{wf}) and the other part being the heat recharged by the flowing water (Q_{wr}). The heat released by the freezing of the layer can be calculated by:

$$\int Q_{wf}dt + L\rho_w h_w + \rho_i c_i h_i(T_i - T_f) \tag{16}$$

where ρ_w and ρ_i are the densities of water and ice (kg/m^3), respectively; t is the freezing time of the layer; c_i is the specific heat of the ice (J kg^{-1} K^{-1}); h_w and h_i are the thicknesses of the water and icing layer(m), respectively; T_i and

T_f are the mean temperatures of the icing layer at the beginning and end of the calculation. The density and specific heat of ice are both functions of temperature. For a 10 K change of temperature, however, the change in ρ_i is very small, therefore, ρ_i is set as constant with a value of 0.92*10^3 kg m^{-3}. For temperatures T_{ice}>150 K, the relationship between specific heat and the temperature is given by Yen (1981):

$$c_i = 2,7442 + 0,1282T_{ice} \tag{17}$$

(note that the c_i has the unit of J mol^{-1} K^{-1} and T_{ice} is in K). Thus, the heat generated by flowing water for an icing cycle can be estimated through (15), (16), and (17). Finally the energy budget for entire period of an icing cycle becomes:

$$\int Q_{wr} + \int Q_{wf} = \int Q^* - \int(Q_h + Q_e + Q_{il} + Q_{sa}) \tag{18}$$

RESULTS

ENERGY BUDGET

The total incoming energy for a single icing layer is provided by the heat carried by running water ($\int Q_{wr}$), the latent heat released by the freezing of still water ($\int Q_{wf}$), and the heat generated by the absorption of solar radiation ($\int Q_{sa}$). This energy will be liberated into the atmosphere and conducted into the underlying ice body in terms of sensible heat ($\int Q_h$), the latent heat of evaporation/sublimation ($\int Q_e$), the radiative heat loss ($\int Q^*$) at the surface, and the heat conduction into underlying ice ($\int Q_{il}$). When a full icing layer cycle is considered, $\int Q_{il}$ is a complicated component of the energy budget. Depending on the temperature regime of the underlying ice body previous to overflow and the weather conditions during the event, this conduction may either as a energy contribution or dissipation. Table I gives the energy budgets for six icing layer events as well as their duration, thicknesses, mean air temperatures and wind speeds during their formation. The thickness of icing layers varies from 2 to 8.1 cm, and the mean air temperatures during the formation of each icing layer range from -3.5 °C to -29.5 °C.

For convenience, Table II provides the proportion of the energy components in terms of incoming and dissipative energy. Among the energy supply terms of $\int Q_{wr}$ (heat carried by running water), $\int Q_{wf}$ (latent heat released by the freezing of the still water layer) and $\int Q_{sa}$ (heat generated by absorption of solar radiation), $\int Q_{wr}$ contributes a significant amount of energy under the warmer temperature regime. The relative amount can be more than 60 % of the total incoming energy, as was shown in the case of icing events 1 and 2. As the air temperature decreases, the percentage contribution of $\int Q_{wr}$ simultaneously decreases. When the mean air temperature during an icing event is lower than -2 °C, the percentage of $\int Q_{wr}$ is reduced to less than 8 %, as seen in icing events 5 and 6. Conversely, the contribution of $\int Q_{wf}$ increases when temperature decreases. For example, in event 6 when the mean air temperature is -29.5 °C, the latent heat released from the freezing of the still water con-

TABLE I

The physical characteristics, weather conditions and energy budgets of six icing layers

	Icing Event					
Term	No. 1	No. 2	No. 3	No. 4	No. 5	No. 6
Duration (hr)	12.50	11.17	37.50	14.33	14.17	17.00
Thickness (cm)	2.0	3.5	8.1	4.2	5.3	5.0
T_{mean} (°C)	-3.5	-4.1	-5.7	-14.4	-22.0	-29.5
U_{mean} (m/s)	15.7	14.6	16.7	4.6	13.0	5.9
Total sensible heat (J/m^2) $\times 10^3$	-1235.7	-866.8	-4831.4	-1141.4	-4119.7	-3523.6
Total latent heat (J/m^2) $\times 10^3$	-251.7	-92.7	-808.9	-907.8	-1347.5	-1176.9
Total heat conduction (J/m^2) $\times 10^3$	193.6	-61.6	-3713.6	-990.7	1300.2	-615.1
Total absorbed solar radiation (J/m^2) $\times 10^3$	169.8	167.8	2392.5	71.6	15.1	866.0
Total heat brought by running water (J/m^2) $\times 10^3$	798.0	431.3	2471.1	336.3	245.7	134.0
Total latent heat from freezing of still water layer (J/m^2) $\times 10^3$	136.8	97.4	739.6	210.9	1381.4	1932.2
Net radiation (J/m^2) $\times 10^3$	-189.2	-324.6	-3750.7	-2421.0	-2524.8	-2383.4

TABLE II

The energy budgets for six icing layers in percentages: (a) energy dissipation terms; (b) energy supply terms

(a)	Icing Event					
Term	No. 1	No. 2	No. 3	No. 4	No. 5	No. 6
Sensible heat (%)	73.7	64.4	36.9	21.0	51.5	45.8
Latent heat (%)	15.0	6.9	6.2	16.6	16.9	15.3
Net radiation (%)	11.3	24.1	28.6	44.3	31.5	30.9
Heat conduction (%)		4.6	28.3	18.1		8.0
(b)	Icing Event					
Term	No. 1	No. 2	No. 3	No. 4	No. 5	No. 6
Heat from running water (%)	61.5	80.3	44.1	50.7	8.1	6.5
Heat from freezing of still water layer (%)	10.5	7.2	13.2	34.1	47.0	65.9
Heat from solar radiation (%)	13.1	12.5	42.7	15.2	0.7	27.5
Heat from conduction (%)	14.9				44.2	

tributes up to 65.9 % of the total incoming energy. When the temperature is -3.5 °C, the slower growth rate of the ice allows for prolonged intra-layer runoff and the contribution from $\int Q_{wf}$ is only about 10 %. These relationships are illustrated in Figure 5. Nevertheless, in all cases, most of the energy is provided by water associated heat ($\int Q_{wr}+\int Q_{wf}$), accounting for 55 % to 85 % of the total energy input.

Solar radiation provides the other primary source of incoming energy. The relative amount, however, depends completely on the time of the overflow. A strong relative contribution (up to 42 %) can be expected if a large part of the layer forms during daylight, as in event 3. Occasionally, heat conduction from the underlying ice also contributes energy to the icing layer. This happens primarily when air temperature decreases rapidly during icing formation, the temperature of the new icing layer drops quickly, creating a situation where the temperature of the underlying ice is warmer than that of the icing layer. In most situations, however, the heat is conducted into rather than out of the underlying ice.

Sensible heat plays the most important role in energy loss, accounting for 37-74 % of the energy released. In only one case (event 4), when wind speeds were very low throughout the period of icing layer formation, did sensible

heat loss fall to 21 %. In this case, the radiation heat was the dominant means of energy dissipation (44 %). Radiation heat loss is usually secondary in importance, ranging from 11 to 31 % of the total energy loss. Conductive heat losses vary from 8 to 28 %, while the latent heat of evaporation/sublimation is usually the least important, accounting for 6 to 17 % of the total energy loss.

ENERGY BALANCE PROCESSES DURING ICING LAYER GROWTH

Figure 6 summarises the variation in weather conditions, the temperatures at various depths in the ice, and the energy balance components during the formation of icing layer event 5. The energy balance during the growth of an icing layer is calculated from Equation (15). In these calculations, Q^* is measured while Q_h, Q_e, Q_{il}, and Q_{sa} are all determined in accordance with their governing equations. The term Q_w, heat introduced by water, is difficult to separate from the heat storage, therefore Q_w and ΔQ are treated together as the residual of Equation (15).

When an overflow event occurs, the surface temperature and vapour pressure immediately reach their highest values. Every energy loss term, that is, sensible heat, latent heat
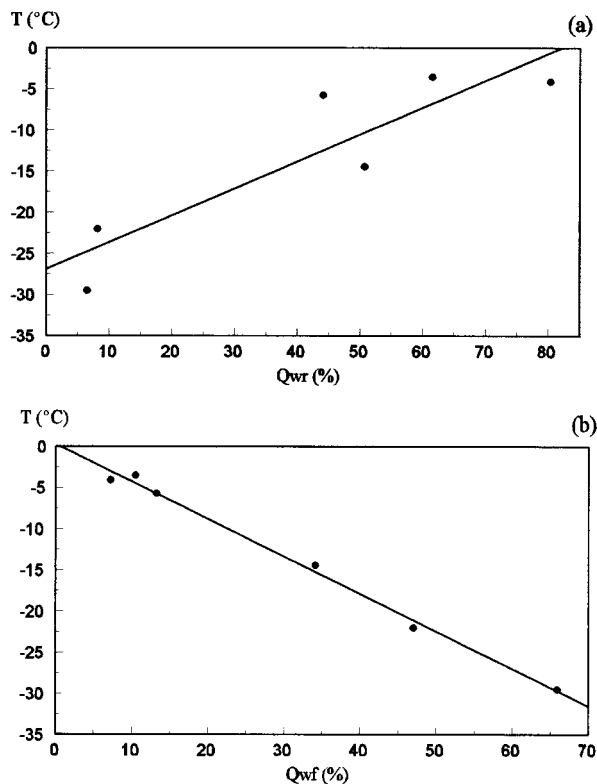
FIGURE 5. The relationships between (a) air temperature [T(EC)] and heat carried by running water [$H_{wr}(\%)$]; (b) air temperature [T(EC)] and heat released by freezing of still water layer [$H_{wf}(\%)$].

Les liens entre (a) la tempérarure de l'air [T(EC)] et la chaleur déplacée par la circulation de l'eau [$H_{wr}(\%)$] ; (b) la température de l'air [T(EC)] et la chaleur libérée par le gel de la couche d'eau stable [$H_{wf}(\%)$].

and conductive heat, also attain their peak values (Fig. 6e). Sensible and latent heat vary in accordance with changes in meteorological variables and the surface temperature of the icing layer. Their values, however, generally tend to decrease with time since the difference in temperatures (ΔT) and vapour pressures (Δq) is also decreasing.

The heat conduction from the underlying ice follows a smoother trend. Once the peak value is reached at the beginning of the cycle, the magnitude of the heat conducted away from the icing layer decreases as the result of the decreasing temperature of the new surface layer, and the increasing temperature of the underlying ice. This trend continues until the temperature difference between the top icing layer and the ice layer below is zero. Heat conduction then becomes positive, and the heat is thus conducted into the new icing layer. The magnitude of the heat conduction during this period increases as the temperature of the top layer decreases. The heat that was stored during the early period is now gradually released. If air temperatures previous to the icing event are warmer, the temperature of the ice is thus higher. After the overflow event, smaller temperature differences between the new icing layer and the underlying ice result in smaller amounts of heat conduction. In the case of very cold air temperatures prior to the

overflow event, the intrusion of a water layer creates a steep temperature gradient, and the heat conduction is thus very significant. If a second overflow appears before the first one is completely frozen, every heat loss term reaches a second peak. The "normal" heat conduction process is, therefore, disrupted and a turning point occurs, as is shown in Figure 7. The magnitude of the second peak of the conduction, however, is not as great as the first peak, simply because the temperature gradients of the ice body are smaller than before.

VARIATION IN ICE TEMPERATURE DURING ICING LAYER FORMATION

The heat conduction through the ice body underneath a new icing layer is controlled by the temperature gradients of the ice. When an overflow occurs, the temperature variations in the ice follow the same pattern as described by Nakawa (1980), which means the closer the point to the surface, the larger the temperature variation, and the smaller the magnitude of the change as the depth increases. What is unique in our study is that after an immediate increase of the temperature in the ice due to the intrusion of overflow, there is a long period of elevated temperature (Fig. 6d). The ice temperature at a depth of 1 cm below the surface rises immediately after the overflow occurs. Followed by a long period of almost constant value, it starts to decrease only when the whole layer freezes. As the depth increases, the temperatures will still rise at the beginning and drop during the later period, but this change is more gradual; the greater the depth, the smaller the temperature change. At a depth of about 50 cm, however, the temperature of ice will undergo very little change. The temperature gradient of the ice immediately below the new icing layer is biggest at the beginning and gradually becomes smaller over time, producing a gradual corresponding decrease in heat conduction. When the temperature of the top layer is lower than that of the layer underneath, the direction of the heat conduction is reversed. The temperature of the lower layer will decrease when the heat is conducted away from it, but, because of the thicker icing layer on the top, the change is rather gradual.

The change of surface temperature of the new icing layer does not have the same pattern as that of the underlying ice because it is a function of the surface energy balance. Nevertheless, immediately after the overflow event, the surface temperature generally decreases rapidly. The rate of the change gets smaller as the icing layer progressively freezes, and the effect of air temperature on the surface temperature becomes more evident (Fig. 6).

DISCUSSION

During the icing layer formation, snowfall has a profound effect on the energy exchange. In view of the specific thermal properties of newly fallen snow such as higher albedo, lower thermal conductivity and lager surface roughness height, one would expect that the energy balance of an icing layer would certainly be modified. There are two possible situations related to snow that contribute to the formation of
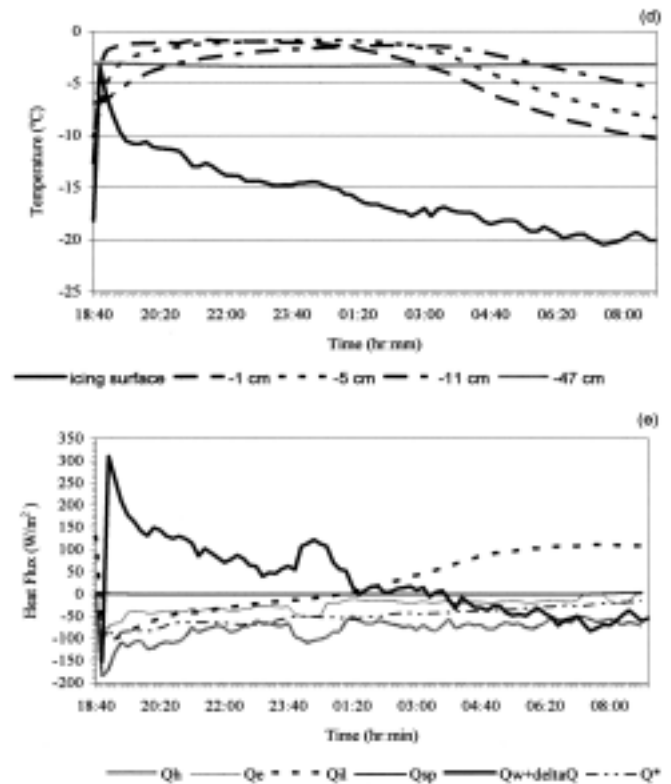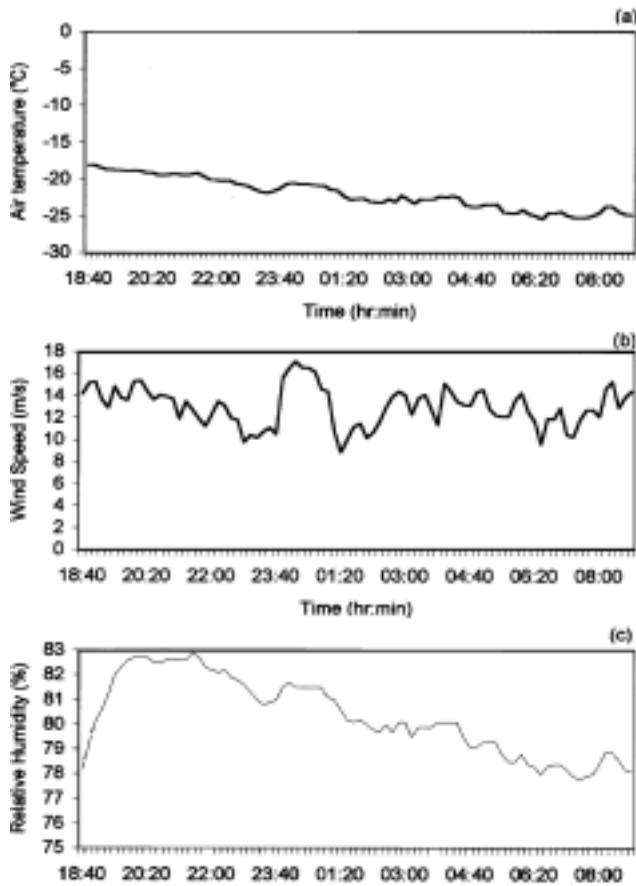
FIGURE 6. The weather conditions, ice thermal conditions and energy balance during an icing layer formation (March 16, 1994). (a) air temperature; (b) wind speed; (c) relative humidity; (d) ice temperatures at different depths; (e) energy balance processes.

Les conditions atmosphériques, les conditions thermiques de la glace et le bilan énergétique pendant la formation de la nappe de glace (le 6 mars 1994) : (a) température de l'air ; (b) vitesse du vent ; (c) humidité relative ; (d) température de la glace selon la profondeur ; (e) bilans énergétiques
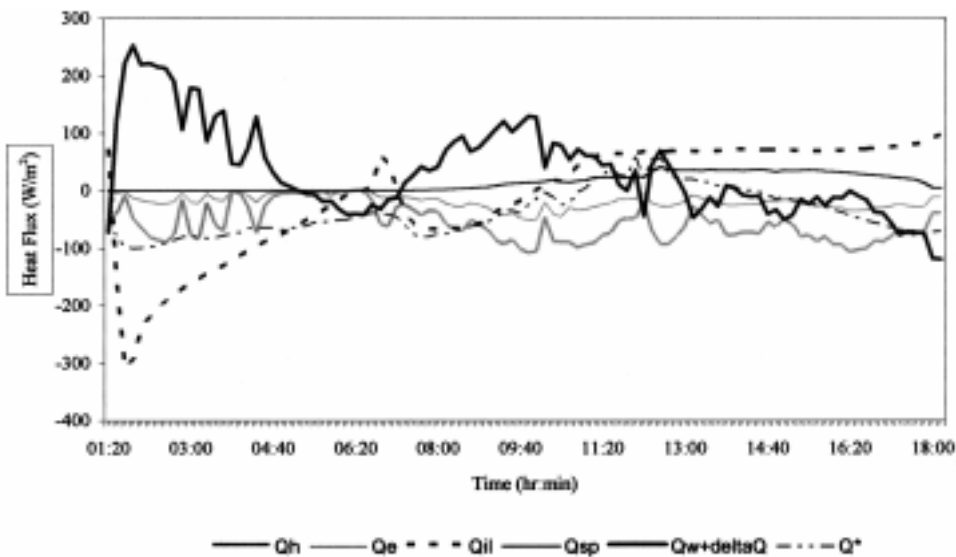

FIGURE 7. The energy balance processes during a double layered icing event (March 19, 1994).

L'évolution du bilan énergétique au cours de la formation d'une double couche de glace (19 mars 1994).

icings. First, snow falls and accumulates after the top layer of the water is frozen. Second, snow exists prior to overflow or falls during the overflow event.

For the first case, the newly fallen snow with high albedo (0.9 to 0.95) (Oke, 1978) and larger bulk extinction coefficient will reduce the penetration of solar radiation. Consequently, the contribution of energy from solar radiation becomes negligible. Although in such a case one of the sources of incoming energy is reduced, because the thermal conductivity of the snow is so much smaller than that of ice (Yen, 1981), the insulating effect of snow will likely prolong the freezing process of the layer. The icing layer can be expected to expand lengthwise for a greater distance.

In the second situation, snow is incorporated directly into the overflow, and a layer of white ice is formed. The albedo of this type of ice is higher than the slush ice but much less than fresh snow, with values falling between 0.6-0.75 (Bolsenga, 1969; Grenfell and Maykut, 1977). Short wave radiation may, therefore, still play a role in icing formation, but the significance of this factor will be reduced. Because water is moving within the snow, some of the heat brought by this water will be used to melt snow crystals, which may also alter the energy balance.

In this paper, we concentrate mainly on the energy exchange processes of icing formation without the incorporation of snow. For the energy balance of overflow when snow plays a role, more research is needed. Also, one of the major concern of this research is the determination of the energy brought by flowing water. Since it is extremely difficult to determine the water volume and flow speed between the ice layers in the filed condition, the energy transferred by flowing water is not able to calculate directly. Instead, the term is estimated through the residual of the energy balance equation. This will certainly introduce an error which is caused by the errors in measurements of meteorological parameters, surface parameters (albedo and roughness) and ice temperatures, and in the estimates of the thermal properties of ice. However, this paper provides a framework of the relative importance of the energy components during icing formation. This is supported by an experimental research (Hu and Pollard, 1997).

CONCLUSION

The formation of icings involves a complex combination of thermodynamics and hydrodynamics. This paper examines the energy exchange processes during icing layer formation under a range of climatic conditions and for different icing layer thicknesses. For thicker icing layers that commonly occur on larger river icings in subarctic areas, the following conclusions can be drawn about the characteristics of the energy exchange.

The energy input for icing layers comes from two sources: water and solar radiation. Under warmer air temperature regimes, about 60-87 % of the heat is supplied by running water while the heat released by the freezing of the water layer contributes only a small proportion. Under colder air temperatures, on the other hand, most of the heat is produced by the latent heat released by the freezing of the water layer. Solar radiation is an important source of incoming energy when snow is not involved. If the icing layer forms during daytime, the absorption of solar radiation can constitute up to 40 % of the total energy. This amount will be greatly reduced if snow is incorporated into the overflow.

Among the terms of energy dissipation, sensible heat loss is generally the most significant and represents about 36 to 74 % of the total energy loss. Radiation heat loss is the second most significant, while latent heat loss is the least important accounting for only 6 % to 17 % of the total energy dissipation.

Heat conduction into underlying ice plays a complex role during a full cycle of icing layer formation. Heat is conducted away from the icing layer in the period immediately after an overflow, and into the layer during the hardening period of the layer. In most cases, it is still primarily a heat loss component within the overall energy budget.

ACKNOWLEDGEMENTS

REFERENCES

Akerman, J. H. 1980. Studies on periglacial geomorphology in West Spitsbergen. Meddelanden Fran Lunds Universitets Geografiska Institution, Avhandlingar, vol. LXXXIX, 297 p.

Bolsenga, S. J. 1969. Total albedo of great lakes ice. Water Resources Research, 5 (5), 1132-1133.

Carey, K. 1973. Icings developed from surface and ground water. CRREL Monograph III-D3, U. S. Army Cold Regions Research and Engineering Laboratory, Hanover, New Hampshire, 67 p.

Environment Canada, 1950-1990. Canadian weather review. Atmospheri c Environment Service, Downsview, Ontario, Canada.

Froehlich, W. and Slupik, J. 1982. River icings and fluvial activity in extreme continental climate: Khangai Mountains, Mongolia. Proceedings, Fourth Canadian Permafrost Conference. National Research Council of Canada, Ottawa, Ontario, p. 203-211.

Gavrilova, M. K. 1972. Radiation and heat balances, thermal regime of an icing. The role of snow and ice in hydrology. Proceedings of Banff Symposia, Sept. 1972. Vol. 1, Unesco, WHO-IAHS, p. 496-504.

Greene, G. M. and Outcalt, S. I. 1985. A simulation model of river ice cover thermodynamics. Cold Regions Science and Technology, 10, 251-262.

Grenfell, T. C. and Maykut, A. 1977. The optical properties of ice and snow in the Arctic basin. Journal of Glaciology, 18(80), 445-462.

Hay, J. E. and Fitzharris, B. B. 1988. A comparison of the energy-balance and Bulk-aerodynamic approaches for estimating glacier melt. Journal of Glaciology, 34(117), 145-153.

Hu, X. and Pollard, W. H. 1997. Ground icing formation: experimental and statistical analyses of the overflow processes. Permafrost and Periglacial Processes. 8, 217-235.

Hobbs, P. V. 1974. Ice physics. Oxford University Press, Oxford.

Kane, D. L. 1981. Physical mechanics of aufeis growth. Canadian Journal of Civil Engineering, 8, 186-195.

Kane, D. L. and Slaughter, C. W. 1972. Seasonal regime and hydrological significance of stream icings in central Alaska. Proceedings of Banff Symposia, Sept. 1972. Vol. 1, Unesco, WHO-IAHS, p. 528-540.

Kuhn, M. 1979. On the computation of heat transfer coefficients from energy balance gradients on a glacier. Journal of Glaciology, 22(87), 263-272.

Maykut, G. A. and Untersteiner, N. 1971. Some results from a time-dependent thermodynamic model of sea ice. Journal Geophysical Research, 76, 1550-1575.

Moore, R. D. 1983. On the use of bulk aerodynamic formulae over melting snow. Nordic Hydrology, 14(4), 193-206.

Munro, D. S. and Davis, J. A. 1978. On fitting the log-linear model to wind speed and temperature profiles over a melting glacier. Boundary Layer Meteorology, 15, 423-437.

Nakawa, M. 1980. Heat exchange at surface of built-up ice platform during construction. Cold Regions Science and Technology, 3, 323-333.

Oke, T. R. 1978. Boundary layer climates. Methuen & Lo Ltd, London.

Perovich, D. K. and Grenfell, T. C. 1982. A theoretical model of radiative transfer in young sea ice. Journal of Glaciology, 28(99), 341-356.

Pollard, W. H. 1983. A study of seasonal frost mounds, North Fork Pass, Northern Interior Yukon Territory. PhD Thesis. University of Ottawa, Ottawa.

Pollard, W. H. and van Everdingen, R. O. 1992. Formation of seasonal ice bodies. In J. C. Dixon, and A. D. Abrahams Periglacial Geomorphology, p. 281-304. John Wiley and Sons.

Price, A. G. and Dunne, T. 1976. Energy balance computations of snowmelt in a subarctic area. Water Resources Research, 12(4), 686-694.

Rogers, R. R. 1979. A short course in cloud physics (2nd edition). Pergamon Press, New York.

Shen, H. T. and Chiang, L. A. 1984. Simulation Of Growth And Decay Of River Ice Cover. Journal of Hydraulic Engineering, 110(7), 958-971.

Slaughter, C. W. 1990. Aufeis formation and prevention. In W. I. Ryan, and R. D. Crissman, Cold Regions Hydrology and Hydraulics, p. 433-458. American Society of Civil Engineers.

Sokolov, B. L. 1978. Regime of naleds. Proceedings, Permafrost, Second International Conference, USSR Contribution, National Academy of Science, Washington, D.C. , p. 408-411.

Sokolov, B. L., Alekseyev, V. P., Markov , M. L. and Kiolotayev, V. I. 1989. Research into icings and icing processes in the USSR: Major results and prospects. Polar Geography and Geology, 13(4), 233-251.

Sutton, O. G. 1953. Micrometeorology. McGraw-Hill Book Company, Inc. New York.

van Everdingen, R. O. 1982. Management of ground water discharge for the solution of icing problems in the Yukon. Proceedings, Fourth Canadian Permafrost Conference. National Research Council of Canada, Ottawa, Ontario. P. 212-226.

———— 1990. Ground water hydrology. In T. D. Prowse, and C. S. L. Ommanney, Northern Hydrology: Canadian Perspectives, NHRI Science Report No.1, p. 77-101. National Hydrology Research Institute, Environment Canada, Saskatoon, Saskatchewan,

Yen, Y.-C. 1981. Review of thermal properties of snow, ice and sea ice. CRREL Report, 81-10. 27 p.